Nature Environment and Pollution Technology
An International Quarterly Scientific Journal

p-ISSN: 0972-6268
e-ISSN: 2395-3454

Vol. 19 | No. 1 | pp. 295-302 | 2020

Original Research Paper | Open Access

Numerical Investigation of Heterogeneous Nucleation of Supersaturated Water Vapour on Coal-fired PM_{10}

Ju Gao, Ting-fang Yu†, Run-guo Chen, Hao-jie Zhang and Lin Wang
†School of Mechanical and Electrical Engineering, Nanchang University, Jiangxi, Nanchang 330031, China
†Corresponding author: Ting-fang Yu

Nat. Env. & Poll. Tech.
Website: www.neptjournal.com

Received: 16-06-2019
Accepted: 24-07-2019

Key Words:
Heterogeneous nucleation
Coal-fired PM_{10}
Critical supersaturation
Nucleation rate

ABSTRACT

The kinetic model is adopted to describe heterogeneous nucleation of supersaturated water vapour on coal-fired PM_{10}. To verify the accuracy of the kinetic model, it is compared with the Fletcher model and experimental data. Additionally, the comparison for condensation and evaporation coefficients and the relative importance of two diffusion condensation mechanisms are systematically analysed during embryo growth process. Furthermore, the influence of vapour temperature on nucleation rate and critical supersaturation for coal-fired PM_{10} are researched. The results show that the predicted critical supersaturation for Kinetic model is far closer to the experimental data compared with the Fletcher model. What is more, once the embryo radius rn reaches to the critical embryo radius r*, it can grow spontaneously, and the indirect surface diffusion mechanism is more important than the direct addition mechanism to embryo growth, the value of RTO is always above 100. It is also found that increase in the vapour temperature is conductive to nucleation process, which can increase the nucleation rate and decrease the barrier of nucleation free energy.

INTRODUCTION

The frequent haze weather has attracted people's extensive attention to the particulate matters in recent years (Siddharth et al. 2008). Coal-fired power plants are one of the main sources for particulate matter in the atmosphere environment (Liu et al. 2016). These particles can not only cause serious environmental problems but also pose a serious threat to people's health. Particles with the diameter less than 10 microns can enter the respiratory system of the human body, causing damage to the heart and lung functions, resulting in arrhythmia, myocardial infarction, heart failure, atherosclerosis and other diseases (Bentayeb et al. 2012).

However, conventional particle abatement devices such as cyclone separator, water scrubber, fabric filters, electrostatic precipitator and so on have less effective in collecting submicron particles (Hu et al. 2018, Zhou et al. 2016). Therefore, to find a valid preconditioning method to improve the removal efficiency for fine particles has become an urgent problem. Heterogeneous condensation as a promising preconditioning technique has been widely used in the traditional particle separation processes (Heidenreich et al. 1995, Hao et al. 2016). At present, a large number of experimental and theoretical researches focus on the removal efficiency for fine particles by means of vapor heterogeneous condensation technology, while ignoring the heterogeneous nucleation process at the initial stage of heterogeneous condensation of water vapor (Hao et al. 2016, Zhou et al. 2016, Wen et al. 2014). Fan et al. (2013) pointed out that the whole process for heterogeneous condensation include three stages: nucleation, transition and growth stage. The heterogeneous nucleation stage plays an important role in the process of steam heterogeneous condensation, so it is of great significance to study the heterogeneous nucleation characteristics for supersaturated steam on particle surface.

Studies on heterogeneous nucleation have a long history. Fletcher (1958) was the first to study heterogeneous nucleation of vapor on insoluble spherical particles, which contained the effect of particle size. Fan et al. (2007) numerically investigated the water vapor (with or without wetting agents) on $PM_{2.5}$ heterogeneous nucleation behaviour according to Fletcher's classical nucleation theory. However, Chen et al. (2000) revealed that the prediction of critical supersaturation for Fletcher classical nucleation theory was flawed, which was too high compared with experimental data. In recent years, the kinetic model has been widely used to investigate heterogeneous nucleation of supersaturated vapor on particles. Luo et al. (2014) derived the growth rate for the cap shaped embryo formed on the particle surface based on the kinetic nucleation model. Fan et al. (2015) put forward to a modified expression for the steady-state heterogeneous nucleation rate based on the kinetic model and validated the advantage of the expression. All these researches indicate that the kinetic model is a valid tool to investigate the phenomenon for heterogeneous nucleation of supersaturated water vapor on particle.

In this paper, we apply the kinetic model (Luo et al. 2014), in which three factors are taken in account, including the effect of line tension, two mechanisms of embryo growth and coal-fired PM_{10} surface wettability, to research the heterogeneous nucleation characteristics of supersaturated vapor on spherical coal-fired PM_{10}. In addition, the effects of operational parameters including temperature and supersaturation of vapor on heterogeneous nucleation parameters are also investigated.

Physical Model

Fig.1 shows the growth process of embryo formed on coal-fired PM_{10} surface. The embryo can grow via the condensation of water vapor molecules direct diffusion from the vapor phase and the indirect diffusion for particle surface absorbed water at the rate of $C_n(\alpha)$ and $C_n(\beta)$, respectively. Meanwhile, condensation and evaporation occur simultaneously, the embryo droplet could also shrink by evaporation of water molecules to both the vapor phase and particle surface at the rate of $E_n(\alpha)$ and $E_n(\beta)$, respectively.

Fig. 2. shows the process of the number changes for embryo. The number of embryos formed on particle surface per unit area is defined as f_n and the change rate of f_n is written as:

$$\frac{df_n}{dt} = C_{n-1} f_{n-1} - \left(C_n + E_n\right) f_n + E_{n+1} f_{n+1} \quad \ldots(1)$$

Where, C_n and E_n denote the coefficients of condensation and evaporation for embryo droplet, respectively.

When we take into account the effect of line tension in kinetic nucleation model, the free energy for forming an embryo on coal-fired PM_{10} is given by (Luo et al. 2014).

$$\Delta G = \Delta G_v V + \sigma_{lv} S_{lv} + \left(\sigma_{sl} - \sigma_{sv}\right) S_{sl} + \tau L_{scv} \quad \ldots(2)$$

Where, V is the volume of embryo droplet (m^3), ΔG_v represents the free energy difference between vapor phase and liquid phase unit volume ($J \cdot m^{-3}$), σ_{ij} ($N \cdot m^{-1}$) is the surface free energy between phase i and j, and S_{ij} is the surface area of the interface (m^2). τ (N) is the line tension at the triple phase boundary between embryo, substrate, and vapor phase and L_{scv} is the total length for the three-phase contact line (m).

From Fig. 1, the geometric parameters are written as:

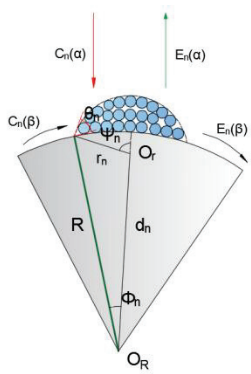

Fig. 1: Schematic diagram for the growth process of embryo.

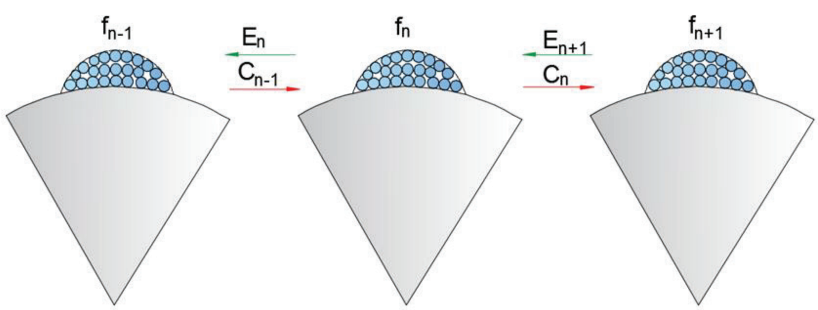

Fig. 2: Kinetic process for the change rate of the embryo number.

$$V=\frac{1}{3}\pi r_n^3\left(2-3\cos\psi_n+\cos\psi_n^3\right)$$
$$-\frac{1}{3}\pi R^3\left(2-3\cos\Phi_n-\cos\Phi_n^3\right) \quad \ldots(3)$$

$$S_{lv}=2\pi r_n^2\left(1-\cos\psi_n\right) \quad \ldots(4)$$

$$S_{sl}=2\pi R^2\left(1-\cos\Phi_n\right) \quad \ldots(5)$$

$$L_{scv}=2\pi r_n\sin\psi_n \quad \ldots(6)$$

$$d=\sqrt{r_n{}^2+R^2-2mr_nR} \quad \ldots(7)$$

$$\cos\psi_n=\frac{mR-r_n}{d} \quad \ldots(8)$$

$$\cos\Phi_n=\frac{R-r_n m}{d} \quad \ldots(9)$$

Where, r_n represents embryo radius (m), R is the radius of coal-fired particle (m), d is the distance between the centre of embryo droplet and that of particle (m), m is the cosine of microscopic contact angle θ_n.

The microscopic contact angle θ_n is a function of line tension τ and macroscopic contact θ_∞ (Hienola et al. 2007).

$$\cos\theta_\infty=\cos\theta_n+\frac{\tau\left(R-r\cos\theta_n\right)}{\sigma_{lv}r_nR\sin\theta_n} \quad \ldots(10)$$

The radius of the critical embryo is:

$$r_n^*=\frac{2\sigma_{lv}V_{wm}}{k_BT\ln S} \quad \ldots(11)$$

Where, k_B is the Boltzmann constant (1.38×10^{-23} J·K^{-1}), T (K) is the temperature of water vapour, V_{wm} is the volume of a water molecule (m^3), S is water vapour supersaturation, which is the ratio of the ambient vapour pressure to saturation vapour pressure.

The heterogeneous nucleation free energy barrier corresponds to the maximum value of ΔG, which is the formation energy for the critical embryo (Hienola et al. 2007).

$$\Delta G^*=\frac{2\pi r^{*2}\sigma_{lv}}{3}f\left(m,x\right)+2\pi R\tau\left(\frac{1-\cos\Phi_n}{\sin\Phi_n}\right) \quad \ldots(12)$$

Where, $f(m,x)$ is the geometrical factor (Fan et al. 2007).

The expression of condensation coefficient in the kinetic model for embryo is (Xu et al. 2017):

$$C_n=C_n\left(\alpha\right)+C_n\left(\beta\right) \quad \ldots(13)$$

$$C_n\left(\alpha\right)=\alpha_n\frac{p_v}{\sqrt{2\pi m_{wm}k_BT}}S_{cv}\left(r_n\right) \quad \ldots(14)$$

$$C_n\left(\beta\right)=N_1\nu\delta\exp\left(-\frac{\Delta G_{diff}}{k_BT}\right)L_{cvs}\left(r_n\right) \quad \ldots(15)$$

$$N_1=\frac{p_v}{\nu\sqrt{2\pi m_{wm}k_BT}}\exp\left(\frac{\Delta G_{des}}{k_BT}\right) \quad \ldots(16)$$

Where, P_v is the ambient pressure of water vapor (Pa), ν denotes the vibration frequency of one molecule on the surface (s^{-1}), δ is the mean jump distance for one water molecule (m), ΔG_{diff} is the surface diffusion energy for one water molecule (J), α_g denotes the sticking coefficient of embryo droplet. N_1 is the surface concentration of water molecules. ΔG_{des} is the desorption energy for individual water molecule (J).

The explicit expression of evaporation coefficient is written as (Fan et al. 2015):

$$E_n=E_n\left(\alpha\right)+E_n\left(\beta\right) \quad \ldots(17)$$

$$E_n\left(\alpha\right)=\exp\left(\frac{2\sigma V_{wm}}{k_BTr_n}\right)\frac{P_v^{sat}}{\sqrt{2\pi m_{wm}k_BT}}S_{cv}\left(r_n\right) \quad \ldots(18)$$

$$E_n\left(\beta\right)=\exp\left(\frac{2\sigma V_{wm}}{k_BTr_n}\right)\delta N_1^{sat}\nu\exp\left(\frac{\Delta G_{diff}}{k_BT}\right)L_{cvs}\left(r_n\right) \quad \ldots(19)$$

The heterogeneous nucleation rate is one of crucial parameters to research heterogeneous nucleation process and the expression of nucleation rate is (Fan et al. 2015):

$$J=Z\cdot\left[C_n^*\left(\alpha\right)+C_n^*\left(\beta\right)\right]\cdot\exp\left(-\frac{\Delta G^*}{k_BT}\right) \quad \ldots(20)$$

and

$$Z=\sqrt{\frac{\sigma}{k_BT\left(2+\cos\psi_{n^*}\right)}\cdot\frac{V_{wm}}{\pi r_{n^*}^2\left(1-\cos\psi_{n^*}\right)}} \quad \ldots(21)$$

Table 1: Parameters for the coefficients of condensation and evaporation in heterogeneous nucleation on coal-fired particle.

Parameter	Symbol	Value
Mean jump distance	δ (nm)	0.32
Line tension	τ (N·m^{-1})	-1×10^{-11}
Macroscopic contact angle	θ_∞ (°)	40
Surface diffusion energy	ΔG_{diff} (J·molecule^{-1})	2.9×10^{-21}
Desorption energy	ΔG_{des} (J·molecule^{-1})	2.9×10^{-20}

Where, Z is the Zeldovich non-equilibrium factor, the superscript '*' denotes the parameters for critical embryo.

The parameters that we used in the kinetic model is listed in Table 1 (Fan et al. 2019 & Xu et al. 2017).

RESULTS AND DISCUSSION

Comparison with the Experimental Data

When the heterogeneous nucleation rate J = 1 s^{-1}, the supersaturation is defined as critical supersaturation, which is the minimum barrier to form a new phase from vapor phase. Fig. 3 shows the comparison of predicted critical supersaturation for Fletcher model (Fletcher 1956) and kinetic model (Luo et al. 2014) with the experimental data (Chen et al. 2000) in heterogeneous nucleation of water vapor on SiO_2 particles. It is found that compared with Fletcher model, the predicted critical supersaturation for kinetic model is much closer to the experimental data. Our prediction results are more consistent with the experimental data for small particles. With the increase of particle size, the prediction data for kinetic model are a little larger than the experimental data, which may be accounted by the roughness of particles.

Contribution of Two Diffusion Mechanisms to Embryo Growth

To investigate the relative importance of the two mechanisms to embryo growth, we define a dimensionless number *RTO* as:

$$RTO = C_n(\mathrm{a}) / C_n(\mathrm{b}) \quad \ldots(22)$$

Fig. 4 shows the variations of *RTO* with particle diameter and embryo radius. The temperature for supersaturated water vapour is 40°C (313.15K), the supersaturation is 1.2, and under this condensation the critical embryo radius r^* is about 5.31nm. It is found from Fig. 4 that when $r_n < r^*$, the particle surface diffusion mechanism plays a dominant action in embryo growth and the value of *RTO* is always above 100. Additionally, for a given particle diameter, the value of *RTO* decreases remarkably with the increasing of embryo radius, which indicates that the mechanism of direct diffusion condensation begins to make more contributions to embryo growth. All these results indicate that the surface diffusion mechanism is more important than the direct addition mechanism when the embryo radius is less than critical embryo radius, and the direct diffusion mechanism plays a significant contribution to the growth of embryo with the increase of embryo size, which is consistent with the conclusion of Fan et al. (2019).

Coefficients of Evaporation and Condensation

Fig. 5 shows the variation of the coefficients of evaporation and condensation with the radius of embryo under different temperatures. It is found that the coefficients of evaporation and condensation increase nearly linearly with the increase of embryo radius r_n. When the embryo radius is less than the

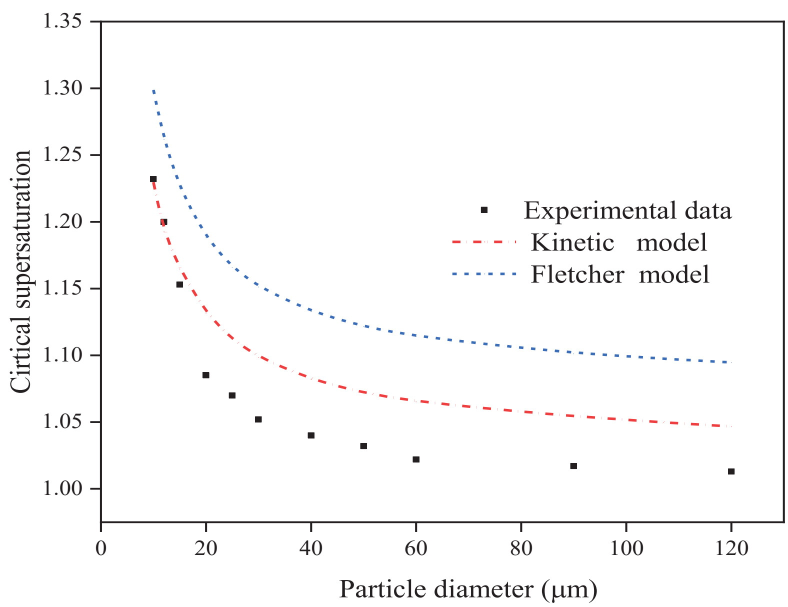

Fig. 3: Comparison with the experimental data.

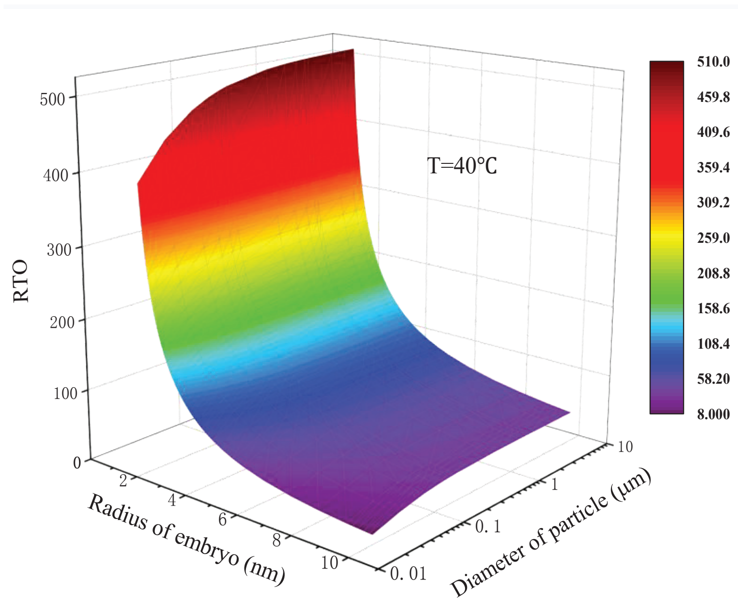

Fig. 4: Variations of *RTO* with particle diameter and embryo size.

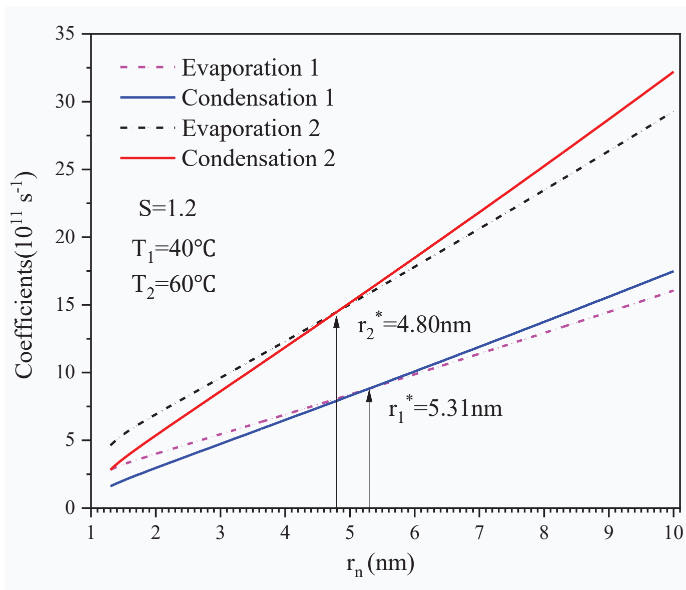

Fig. 5: Variations of evaporation and condensation coefficients with embryo radius.

critical embryo radius $r_n < r^*$, the evaporation coefficient is larger than condensation coefficient and the formed embryo tends to disappear. When $r_n > r^*$, the evaporation coefficient is less than condensation coefficient and the formed embryo tends to be larger. When $r_n = r^*$, the value of evaporation coefficient is equal to condensation coefficient, which means that the embryo is in metastable state and the size of the embryo keeps constant.

Moreover, with the increase of temperature, the value of evaporation and condensation coefficients are enlarged and the laws between them remain the same at different temperatures, which manifests that the improvement of vapour temperature can accelerate the growth of embryo and benefit the heterogeneous nucleation process.

Nucleation Rate

Nucleation rate refers to the number of critical embryos formed on coal-fired PM_{10} surface unit time. Fig. 6 shows that the nucleation rate varies with supersaturation at different particle surface. It can be seen from Fig. 6(a) that the nucleation rates increase exponentially with the increase of supersaturation for a given particle diameter. In the case of particles with the diameter of 2.5 microns, the nucleation rate increases from 6.5×10^5 to 6.9×10^{18}, when the supersaturation increases from 1.2 to 1.3. This is because the increase of supersaturation can reduce the free energy barrier of nucleation and decrease the size of critical embryo radius. Additionally, with the increase of supersaturation, the number of water vapor molecules around the particles is further increased, and there will be more water vapor molecules condensed on particle unit time, all these reasons can account for the changes of nucleation rate.

Fig. 6(b) shows the variations of nucleation rate with vapor supersaturation under different temperatures. It is found that nucleation rate is increased with temperature when the supersaturation is constant. With the temperature increased from 313.15K to 333.15K, the nucleation rate is increased from 1.39×10^{25} to 3.45×10^{26} under the condition S = 1.5. This is because the improvement of temperature can dramatically increase the diffusion condensation rates for water vapor molecules and decrease the surface tension of embryo droplet. Furthermore, as the supersaturation to be larger, temperature is not the dominant factor to affect the condensation rate and the increase of temperature is not obvious to accelerate the improvement of nucleation rate.

Critical Supersaturation

Fig. 7 shows the variation of critical supersaturation with particle diameter and temperature. It can be seen from Fig. 7; the critical supersaturation decreases remarkably with the increase of particle diameter when the particle diameter is less than 0.1μm at different temperatures. As the particle diameter becomes larger, the trend of decrease for critical supersaturation tends to level off. Additionally, the critical supersaturation decreases with vapour temperature for a given particle, when the temperature rises from 313.15K (40°C) to 333.15K (60°C), and the critical supersaturation for coal-fired particles with a diameter of 2.5μm is reduced from 1.180 to 1.152. This is because the increase of temperature can not only decrease the critical embryo size, but also reduce the barrier of free energy for heterogeneous nucleation, which can also account for the increase of nucleation rate with the increase of temperature. Therefore, the improvement of temperature is conducive to the occurrence of heterogeneous nucleation of supersaturated vapour on coal-fired PM_{10} surface.

CONCLUSIONS

1. The kinetic model, in which three factors are considered including the effect of line tension, two mechanisms of embryo growth and the wettability of coal-fired PM_{10} can be used to accurately predict the heterogeneous nucleation process.
2. When the embryo radius is less than critical embryo radius $r_n < r^*$, the mechanism of particle surface diffusion plays a dominant action in embryo growth and the value of *RTO* is always above 100.
3. The heterogeneous nucleation rate is very sensitive to

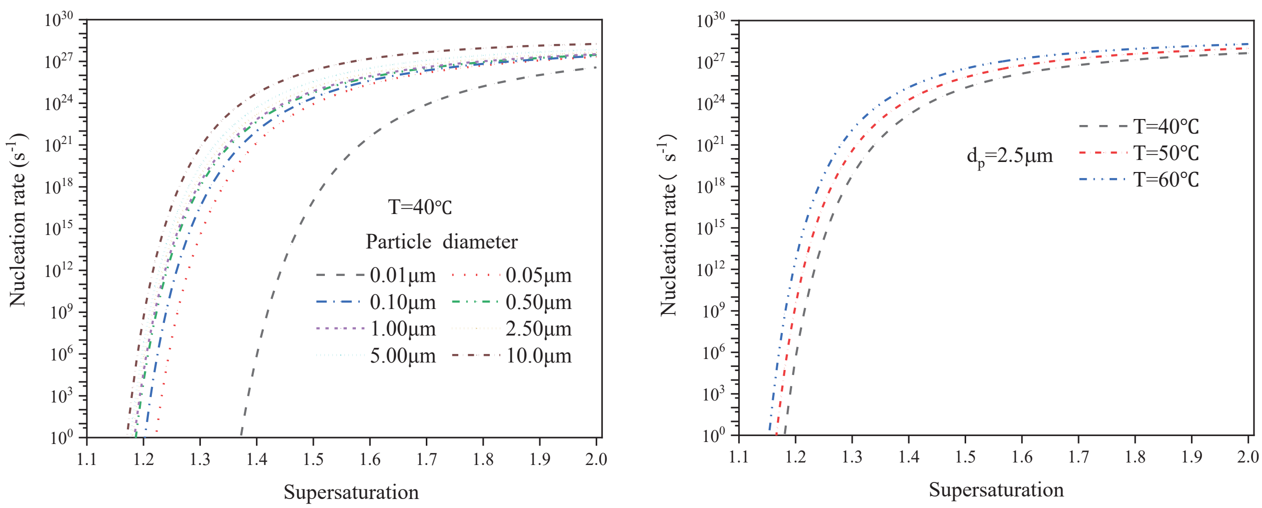

(a) (b)

Fig. 6: Variations of nucleation rate with the supersaturation.

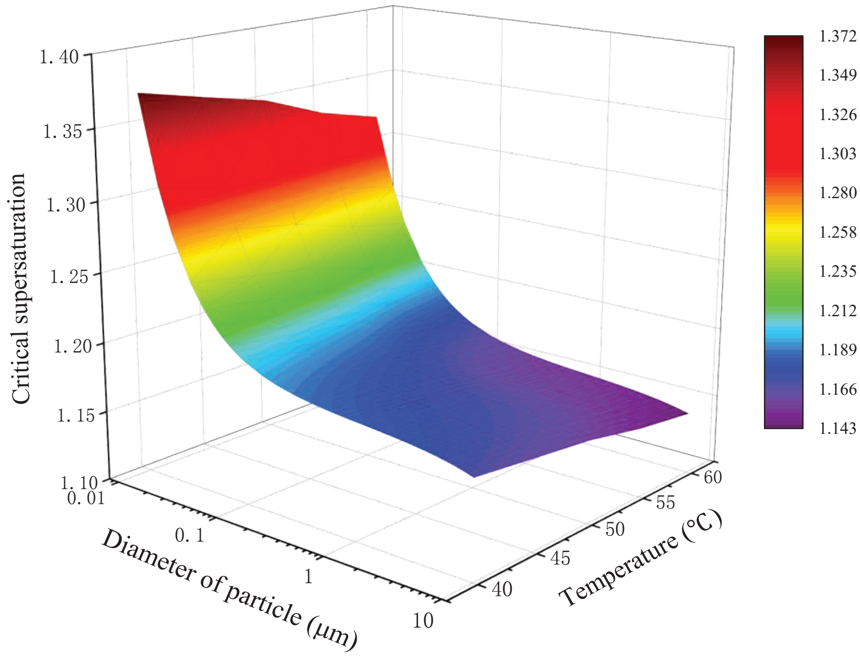

Fig. 7: Variations of critical supersaturation with particle diameter and temperature.

supersaturation, and it increases exponentially with the increase of supersaturation.

4. The critical supersaturation decreases remarkably with the increase of particle diameter when the particle diameter is less than 0.1μm at different temperatures. With the increase of particle diameter, the trend of the decrease of critical supersaturation tends to level off.
5. The improvement of supersaturated vapour temperature can decrease critical embryo size, increase diffusion condensation rates, thereby increasing the nucleation rate then decreasing the critical supersaturation, which is beneficial to heterogeneous nucleation on coal-fired particles.

ACKNOWLEDGEMENT

This study was supported by the National Natural Science Foundation of China (No. 61262048), the Key Research and Development Project of Jiangxi Province (No. 2017ACG70012).

REFERENCES

Bentayeb, M., Simoni, M., Baiz, N., Norback, D., Baldacci, S., Maio, S., Viegi, G. and Annesi-Maesano, I. 2012. Adverse respiratory effects of outdoor air pollution in the elderly. International Journal of Tuberculosis & Lung Disease, 16(9): 1149-1161.

Chen, C.C. and Tao, C. J. 2000. Condensation of supersaturated water vapour on submicrometer particles of SiO_2 and TiO_2. Journal of Chemical physics, 112(22): 9967-9977.

Fan, F. X., Yang, L. J., Yuan, Z. L. and Yan, J. P. 2007. Numerical prediction of water vapour nucleation behaviour on $PM_{2.5}$ from coal combustion. Journal of Chemical Industry and Engineering (China), 58(10): 2561-2566.

Fan, F.X., Zhang, S.H., Peng, Z. B., Chen, J., Su, M. X., Moghtaderi, B. and Doroodchi E. 2019. Numerical investigation of heterogeneous nucleation of water vapour on PM_{10} for particulate abatement. The Canadian Journal of Chemical engineering, 97: 930-939.

Fan, Y., Qin, F. H., Luo, X. S., Zhang, J. S., Wang, J., Gui, H. Q. and Liu, J. G. 2015. A modified expression for the steady-state heterogeneous nucleation rate. Journal of Aerosol Science, 87: 17-27.

Fan, Y., Qin, F.H., Luo, X.S., Lin, LY., Gui, H.Q., and Liu, J.G. 2013. Heterogeneous condensation on insoluble spherical particles: Modeling and parametric study. Chemical Engineering Science, 102: 387-396.

Fletcher, H. N. 1958. Size effect in heterogeneous nucleation. The Journal of Chemical Physics, 29: 572-576.

Hao, W., Pan, D.P., Huang, R.T., Hong, G.X., Bing, Y., Peng, Z.M. and Yang, L.J. 2016. Abatement of fine particle emission by heterogeneous vapour condensation during wet limestone-gypsum flue gas desulfurization. Energy & Fuels, 30(7): 6103-6109.

Heidenreich, S. and Ebert, F.1995. Condensational droplet growth as a preconditioning technique for the separation of submicron particles from gases. Chemical Engineering & Processing, 34(3): 235-244.

Hienola, A. I., Winkler, P. M., Wagner, P. E., Vehkamäki, H., Lauri, A., Napari I. and Kulmala, M. 2007. Estimation of line tension and contact angle from heterogeneous nucleation experimental data. The Journal of Chemical Physics, 126: 094705.

Hu, B., Yang, Y., Cai, L., Yuan, Z.L., Roszak, S. and Yang, L.J. 2018. Experimental study on particles agglomeration by chemical and turbulent agglomeration before electrostatic precipitators. Powder Technology, 335: 186-194.

Liu, Q.Z., Shen, Z.G. and Tao, L.X. 2016. Research on the application of a wet electrostatic precipitator in coal-fired power plant for "Gypsum

Rain" prevention and treatment. Nature Environment and Pollution Technology, 15(3): 867-872.
Luo, X. S., Fan, Y., Qin, F. H., Gui, H.Q. and Liu, J.G. 2014. A kinetic model for heterogeneous condensation of vapour on an insoluble spherical particle. The Journal of Chemical Physics, 024708.
Siddharth, K. Sharma and Gupta, A.B. 2008. Ambient air interactions between particulate matter and gases of combustion. Nature Environment and Pollution Technology, 7(2): 257-260.
Wen, G.S. and Fan, F.X. 2014. Numerical analysis on growth of soluble PM2.5 by vapour heterogeneous condensation. China Environmental Science, 34(5): 1119-1124.
Xu, J. C., Yu, Y., Zhang, J. and Zhong, H. 2017. Kinetics study of droplet growth on surface of coal-fired fine particles. Journal of Southeast University (Natural Science Edition), 47(3): 506-512.
Zhou, D.L., Li, S.Q., Jin, X., Xiong, G.L. and Huang, W. 2016. Experiments and numerical simulations of the removal of fine particles in the coupling field of electrostatic precipitators. Proceedings of the CSEE, 36(2): 453-458.